

Oxidative Leaching of Chalcopyrite by Cupric Ion in Chloride Media

Saleh Rasouli¹  · Behrad Mojtahedi¹ · Hossein Yoozbashizadeh¹

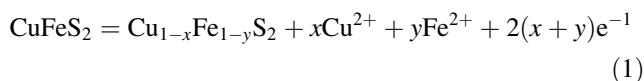
Received: 13 October 2019 / Accepted: 21 January 2020 / Published online: 6 March 2020
© The Indian Institute of Metals - IIM 2020

Abstract In this study, chalcopyrite concentrate produced in Sarcheshmeh copper plant was subjected to oxidative leaching investigation by cupric ion to determine the effect of several parameters on the copper and iron dissolution, including temperature of leaching, time of holding and cupric concentration as oxidant agent in a range of 38–97 °C, 1.5–8.5 h and 0.2–0.8 M, respectively. The leaching media was chloride providing with 3 M HCl 37% and CuCl₂. The experiments were designed by central composite design method. The dissolution of copper and iron was examined. The maximum dissolution of copper 62.64%, was obtained at 85 °C, 7 h and oxidant concentration of 0.7 M. The kinetics model of chalcopyrite leaching and an optimized condition with maximum dissolution of copper and minimum dissolution of iron was obtained by Minitab[®]18 software. Additionally, the thermodynamics of leaching was investigated by Pourbaix diagrams of copper and iron composition, using HSC Chemistry6 software. It was found that the oxidative leaching process is controlled by diffusion through passivation layer with an activation energy of 19.57 kJ/mol.

Keywords Chalcopyrite · Oxidative leaching · Cupric ion oxidant

1 Introduction

Chalcopyrite (CuFeS₂) is the most abundant copper-bearing minerals, near 70% of the Earth's copper reservoir [1]. Today, the most amount of copper is produced through pyrometallurgical processes, but attention has also been paid to hydrometallurgical processing routes due to economical and environmental benefits [2]. Among sulfide minerals of copper, chalcocite (Cu₂S), chalcopyrite (CuFeS₂), covellite (CuS) and bornite (Cu₅FeS₄), chalcopyrite has the lowest rate of leaching [3, 4], meanwhile the hydrometallurgy of chalcopyrite to produce copper is considered to have a less energy consumption rather than the pyrometallurgical method, but there exist matter of thermodynamics and kinetics of reactions [5]. So far, hydrometallurgy process has not been widely used by industrial plants because of the extremely low rate of leaching [6]; hence, there is a need to better understand the kinetics and mechanism of chalcopyrite leaching to improve industrial hydrometallurgical procedure for industrial usage [7]. Several studies, using different acidic media, investigated that the leaching process of chalcopyrite is controlled by the formation of a passive layer and its constitution. Elemental sulfur (S₀), disulfide (S₂²⁻), polysulfides and jarosite are identified as passive layer on chalcopyrite particles [8–13]. There is a model which describes the formation of passive layer as the following reactions [14]:



where $x + y \cong 1$ and $y \gg x$.

Cu_{1-x}Fe_{1-y}S₂ is a middle sulfide phase where leaching rate of this phase is slower than reaction 1:

✉ Hossein Yoozbashizadeh
yoozbashi@sharif.edu

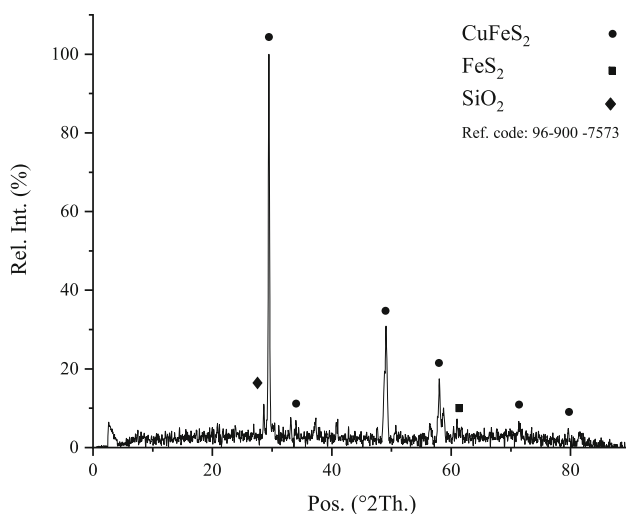
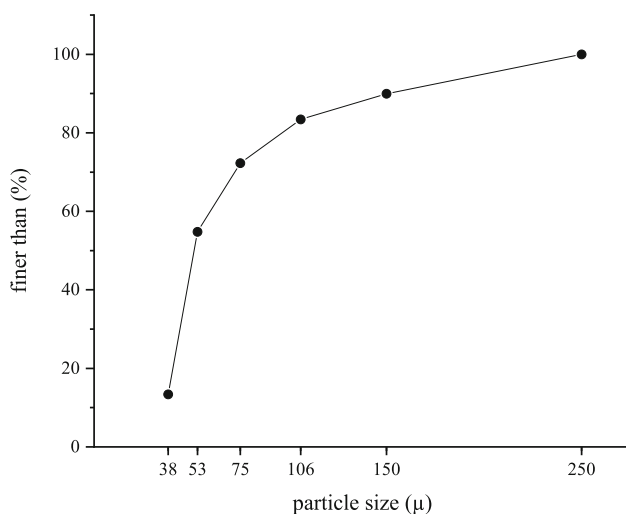
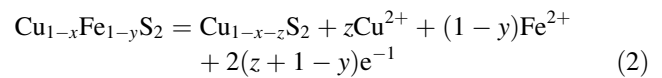
Saleh Rasouli
Saleh.rasouli@gmail.com

Behrad Mojtahedi
behrad.mojtahedi25@student.sharif.ir

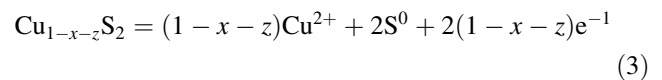
¹ Department of Materials Science and Engineering (Extractive Metallurgy), Sharif University of Technology, Tehran, Iran

Table 1 Chemical analysis of the chalcopyrite concentrate

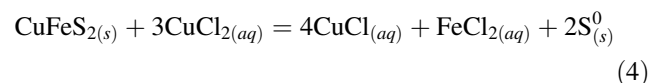
Element	Weight percent (%)
S	36.1
Fe	26.7
Cu	24.56
Si	2.22
Na	1.2
Mg	1
Zn	0.83
Al	0.7
Ca	0.51
Others	Balance

**Fig. 1** XRD pattern of mineral sample**Fig. 2** Seive analysis of chalcopyrite concentrate powder

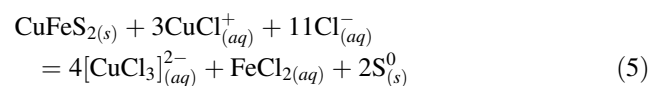
This sulfide phase is one of the causes of formation of passive layer on chalcopyrite during leaching in acidic media. In the next step, leaching of this phase occurs to produce cupric and sulfur, and reaction of this step controls whole of reaction rate:



Several studies have been carried out by different methods for leaching of chalcopyrite: sulfate media leaching [15, 16], chloride media leaching [17–19] and pressure leaching [20] and also different oxidant agents such as Fe^{3+} , H_2O_2 , Cr^{6+} , Ag^+ and Cu^{2+} have been applied to create suitable potential of leaching [21]. Use of chloride media instead of sulfate media reduces the possibility of jarosite formation by elimination of sulfate ions; by the way, the morphology of producing elemental sulfur on the surface of chalcopyrite during leaching is more porous, so a higher rate of leaching is achieved [22]. In addition, the solubility of oxygen in the presence of Cl^- is much more than sulfate media to prepare more oxidative media for leaching. Main advantage of using Cu^{2+} as oxidant agent is that, there is no added impurity to the solution and all of added cupric can be recovered in the next steps of copper production; it is an important issue for industrial plants. In the present research, a chloride solution together with cupric oxidant was prepared by hydrochloric acid and CuCl_2 . Main reaction of leaching in this solution is [23]:



In another study, a similar reaction is suggested as following [24]:



The ratio of $\text{Cu}^{1+}/\text{Cu}^{2+}$ must be less than 1.9 for these reactions to be thermodynamically proceeded [24]. Iron appears as impurity in PLS, and removal of iron needs further treatments. Applying a process with minimum dissolution of iron at its optimum conditions can be impressive and helpful [25]; hence, it necessitates study on the mechanism of the iron dissolution in this process. The present study investigates the effect of temperature, holding time and cupric concentration on the dissolution of copper and iron from chalcopyrite concentrate and provide a model of leaching by Minitab[®] 18 software, and then thermodynamics and kinetics of leaching process are studied.

Table 2 Experimental factors and levels applied in the experiments

Factors	Range and levels				
	− 1.682	− 1	0	+ 1	+ 1.682
Temperature	38	50	68	85	97
Time (h)	1.5	3	5	7	8.5
Cupric concentration (M)	0.2	0.3	0.5	0.7	0.8

Table 3 CCD experimental design

No. test	Time (h)	Temperature (°C)	Cupric conc. (M)	Cu %	Fe %
1	3	50	0.3	19.19	13.42
2	7	50	0.3	28.61	17.46
3	3	85	0.3	40.57	26.69
4	7	85	0.3	51.53	29
5	3	50	0.7	20.47	12.88
6	7	50	0.7	33.35	17.46
7	3	85	0.7	48.89	36.15
8	7	85	0.7	62.64	45.27
9	1.5	68	0.5	34.96	17.04
10	8.5	68	0.5	47.54	19.92
11	5	38	0.5	18.21	7.69
12	5	97	0.5	57.42	40.77
13	5	68	0.2	38.68	17.85
14	5	68	0.8	51.69	35.31
15	5	68	0.5	41.5	25.81
16	5	68	0.5	42.33	24.58
17	5	68	0.5	43.17	21.81

2 Experimental Procedures

2.1 Characterization of Chalcopyrite Concentrate

The chalcopyrite concentrate sample was received from Sarcheshmeh copper plant, Kerman province, at southeast of Iran. The chemical analysis of concentrate is presented in Table 1. Figure 1 shows X-ray diffraction patterns of chalcopyrite sample; besides chalcopyrite, pyrite and silica were major phases. To determine the particle size of concentrate, a sieve analysis was carried out whose results are shown in Fig. 2.

2.2 Leaching Procedure

The leaching experiments were performed under atmospheric pressure in a 250 mL two-necked flask equipped with a reflux condenser and a thermometer. The reaction mixture was heated by a hot plate and agitated by magnetic stirrer. The leaching solution was acidified by hydrochloric

Table 4 ANOVA table for Cu response; (A = temperature, B = time, C = cupric concentration)

Source	DF	Adj SS	Adj MS	F-value	P value
Model	9	0.267139	0.029682	35.51	0
Linear	3	0.256669	0.085556	102.35	0
A	1	0.206978	0.206978	247.60	0
B	1	0.033675	0.033675	40.28	0
C	1	0.016016	0.016016	19.16	0.002
Square	3	0.006553	0.002184	2.61	0.133
A ²	1	0.005570	0.005570	6.66	0.036
B ²	1	0.001286	0.001286	1.54	0.255
C ²	1	0.000019	0.000019	0.02	0.884
Two-way Interaction	3	0.002827	0.000942	1.13	0.401
A*B	1	0.000060	0.000060	0.07	0.797
A*C	1	0.002279	0.002279	2.73	0.143
B*C	1	0.000488	0.000488	0.58	0.470
Error	7	0.005852	0.000836		
Lack-of-Fit	5	0.005712	0.001142	16.39	0.059
Pure Error	2	0.000139	0.00007		
Total	16	0.27991			

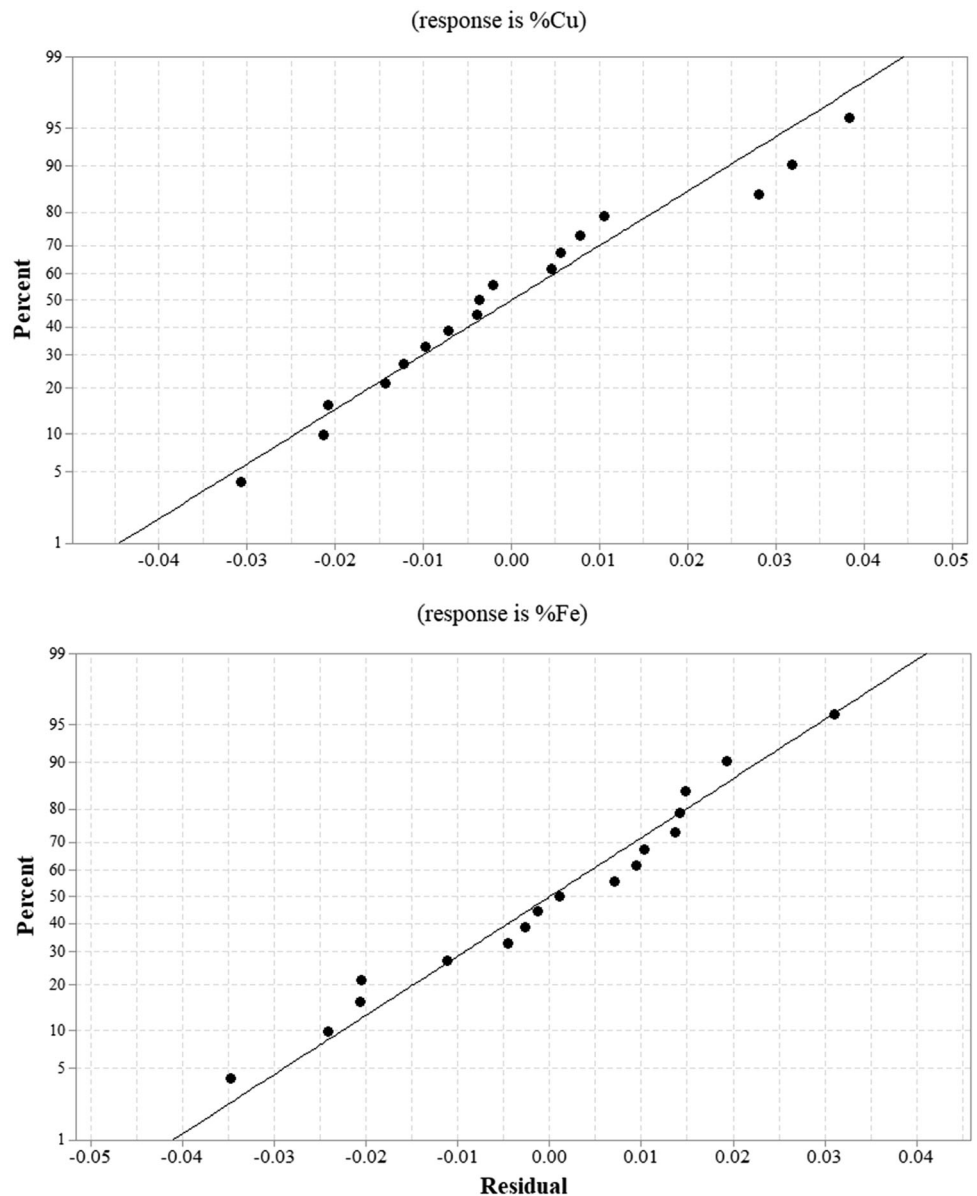
Table 5 Model summary

	R-sq (%)	R-sq(adj) (%)	R-sq(pred) (%)
Full model	97.86	95.10	83.67
modified model	96.27	95.03	91.31

Table 6 ANOVA table for Fe response; (A = temperature, B = time, C = cupric concentration)

Source	DF	Adj SS	Adj MS	F-value	P value
Model	9	0.169008	0.018779	26.43	0
Linear	3	0.151721	0.050574	71.17	0
A	1	0.126519	0.126519	178.05	0
B	1	0.004435	0.004435	6.24	0.041
C	1	0.020767	0.020767	29.23	0.001
Square	3	0.007598	0.002533	3.56	0.075
A ²	1	0.000288	0.000288	0.41	0.545
B ²	1	0.003056	0.003056	4.3	0.077
C ²	1	0.002167	0.002167	3.05	0.124
Two-way Interaction	3	0.009531	0.003177	4.47	0.047
A*B	1	0.000087	0.000087	0.12	0.736
A*C	1	0.008769	0.008769	12.34	0.01
B*C	1	0.000675	0.000675	0.95	0.362
Error	7	0.004974	0.000711		
Lack-of-Fit	5	0.004134	0.000827	1.97	0.37
Pure Error	2	0.000840	0.000420		
Total	16	0.173982			

Fig. 3 Residual plots for Cu(top) and Fe(below) responses



acid. Experiments were carried out at L/S ratio of 10:1, stirring speed of 550 rpm, and acid concentration was set at 3 Molar, based on preliminary tests and experiences.

2.3 Design of Experiments

A response surface methodology was used to study the effect of the variables on the leaching of chalcopyrite. To design experiments, the central composite design (CCD) was carried out. The three factors consisted of four levels and center points of each level; Table 2 shows the levels of factors. The studied factors were using a level of significance of 0.05 (P Value), allowing the detection of interactions between the factors. The statistical analyses of the data were performed by Minitab[®]18 software. Total

experiments of 17 including 3 replicas were considered. Table 3 indicates the experimental design and response of Cu and Fe dissolution percent.

3 Results and Discussion

3.1 Effect of Parameters

Table 4 includes the outputs of standard ANOVA table that are obtained from the statistical software package consisting of all the parameter. As shown in Table 4, central composite design model contains nine terms namely, main effects, square and two-way interactions. Values of “ P -Value” less than 0.05 indicate significant terms of model.

Fig. 4 Main effect plots for Cu dissolution

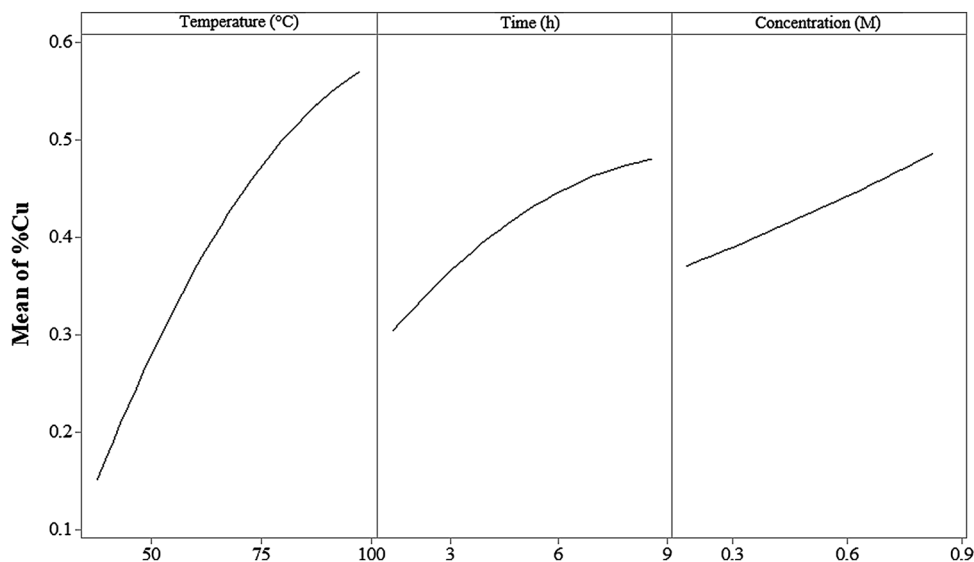
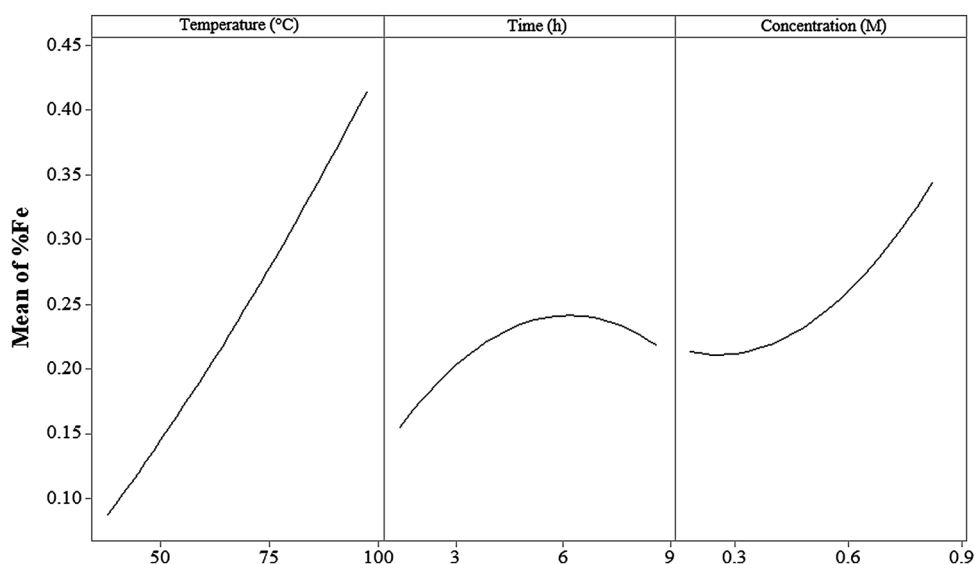


Fig. 5 Main effect plots for Fe dissolution



Equation 6 shows the model of leaching which includes all terms, recommended for uncoded parameters:

$$\begin{aligned} \text{Cu dissolution} = & -0.403 + 0.01389A + 0.0341B \\ & - 0.283C - 0.000072A^2 - 0.00247B^2 \\ & + 0.039C^2 + 0.000078(A)(B) \\ & + 0.0482(B)(C) + 0.00195(A)(C) \end{aligned} \tag{6}$$

which *A* is temperature, *B* is time of holding, and *C* is cupric concentration.

Removing insignificant terms with values of “*P*-Value” more than 0.05 (*B*2, *C*2 and interactions) modifies the model as follows:

$$\begin{aligned} \text{Cu dissolution} = & -0.564 + 0.01568A + 0.02443B \\ & - 0.1779C - 0.000064A^2 \end{aligned} \tag{7}$$

Table 5 indicates model summary of statistical comparison between full model (Eq. 6) and modified model (Eq. 7). It can be seen; full model is more fitted to experimental data although prediction of modified model is much more reliable. Also, standard ANOVA table for Fe response is illustrated in Table 6, *P* values more than 0.05 can be considered as insignificant terms in model of iron dissolution; modified model of Fe dissolution is shown in the following equation:

$$\begin{aligned} \text{Fe dissolution} = & 0.042 + 0.00076A + 0.00888B \\ & - 0.435C + 0.00946A * C \end{aligned} \tag{8}$$

The residual plots for Cu and Fe responses are shown in

Fig. 3 and indicate that errors are extended normally because the residuals are approximately linear. The main effects as illustrated in Fig. 4 have positive effect on dissolution of copper. Among the main parameters, increasing of temperature is more effective compared to holding time and cupric concentration. For Fe dissolution, main effects plot are shown in Fig. 5; generally, the effect of parameters on Fe dissolution is similar to copper dissolution, and temperature has the greatest effect; however, after 6 h, the amount of Fe in solution is decreased.

Due to increase in the pH of solution, initial pH is about -0.47 for 3 M HCl, but as the reactions proceed, acidity of solution is decreased, and this helps to set a condition by maximum dissolution of copper and minimum dissolution of iron. The presence of iron in solution in high amount causes troubles for recovery of copper in next steps of copper production as said before. This condition was determined by Minitab[®] 18, at temperature of $74\text{ }^{\circ}\text{C}$, time of 8.5 h and cupric concentration of 0.33 molar, maximum dissolution of copper occur in the presence of minimum iron. At the optimum condition, copper and iron in leached solution is predicted to be 47.99% and 21.44%, respectively.

Figure 6 indicates interactions between main parameters for iron dissolution. Two non-parallel lines in Fig. 6 show that the effect of one factor depends on the level of the other. This result indicates that iron dissolution is more sensitive to the change of temperature as said before. Additionally, the effect of cupric concentration in lower levels of temperature is negative on iron dissolution and for

the time of 5 and 7 h, influence of cupric concentration on Fe dissolution is approximately the same, although according to Table 6, interaction between temperature and cupric concentration is the only significant interaction term, because of P value less than 0.05.

3.2 Thermodynamics Aspects of the Process

To investigate the thermodynamics of leaching, the Pourbaix diagrams based on Cu and Fe in center point condition are drawn by HSC Chemistry6 and are shown in Fig. 7. This figure illustrates stable area of Cu^{2+} and Fe^{3+} both located in high oxidative potential and low pH. Low initial pH helps the reaction to occur faster but means of pH less than about -0.5 facilitate dissolution of iron that is not suitable for production of copper as said before. After a while, by progressing the reactions and increase in pH, Fe^{3+} will be come unstable and dissolution of iron reduces as shown in Figs. 5 and 6, while cupric ion is still stable. In the preliminary experiments 1 and 2, molar acid concentration was examined, while dissolution of iron was low; however, the rate of chalcopyrite leaching reaction was extremely slow. Using 3 M HCl guarantees both thermodynamics and kinetics aspects of reactions.

3.3 Kinetics of the Process

To investigate the kinetics of reactions, shrinking core model (SCM) was applied, the effect of temperature on reaction rate was examined in the range of $50\text{--}85\text{ }^{\circ}\text{C}$, under the condition of 0.5 M Cu^{2+} and time range of 1–8 h; the

Fig. 6 Interaction effect of main parameters on Fe dissolution

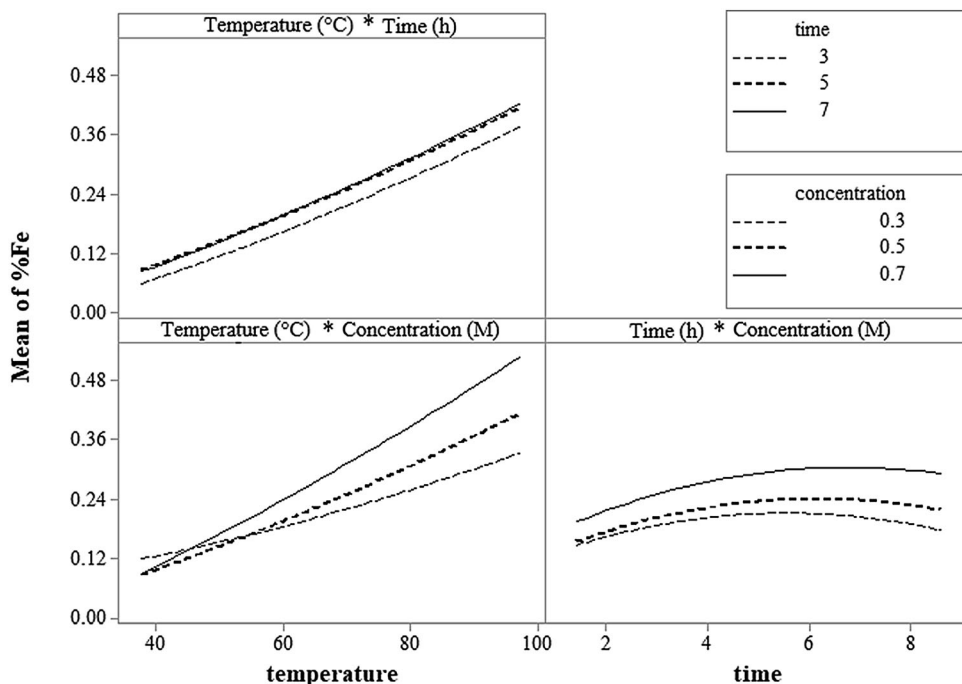
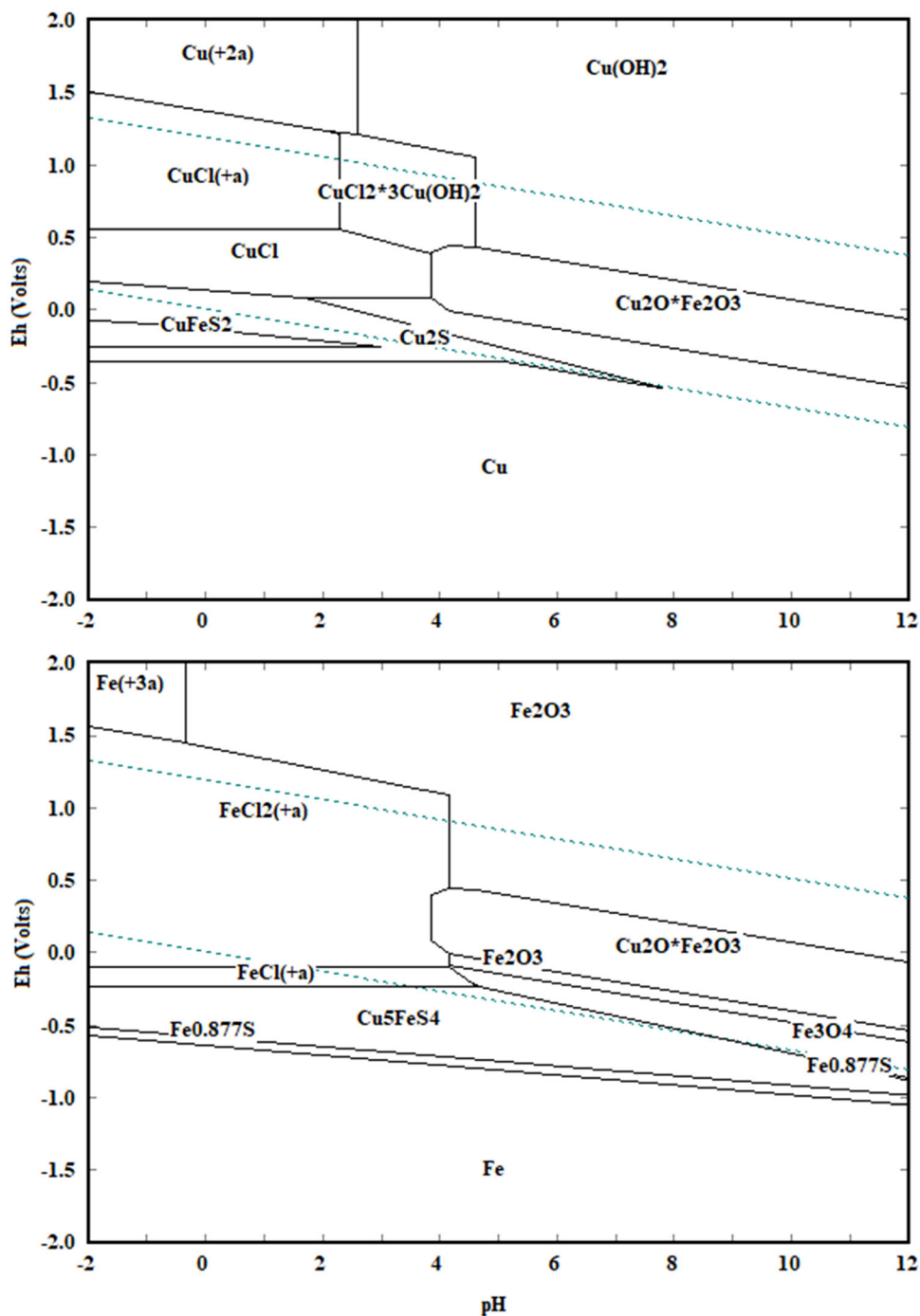


Fig. 7 Pourbiax diagrams based on Cu (top) and Fe (below) dissolution in center point condition



results are shown in Fig. 8. Also, to determine the effect of cupric ion concentration on the reaction rate, several experiments in the range of 0.2-0.8 molar of cupric ions at the temperature of 68 °C at different holding times were carried on, and Fig. 9 indicates the results of these experiments. The experimental data were correlated with different kinetics models. The following equations were examined but they did not fit the experimental data well [26, 27]:

$$1 - (1 - X)^{1/2} = kt \tag{9}$$

$$1 - (1 - X)^{1/3} = kt \tag{10}$$

$$\left[1 - (1 - X)^{1/3}\right]^2 = kt \tag{11}$$

As shown in Figs. 10 and 11, the following diffusion-controlled kinetics equation is found to fit the experimental data with a R-square more than 0.99 for different temperatures and cupric ion concentration, respectively:

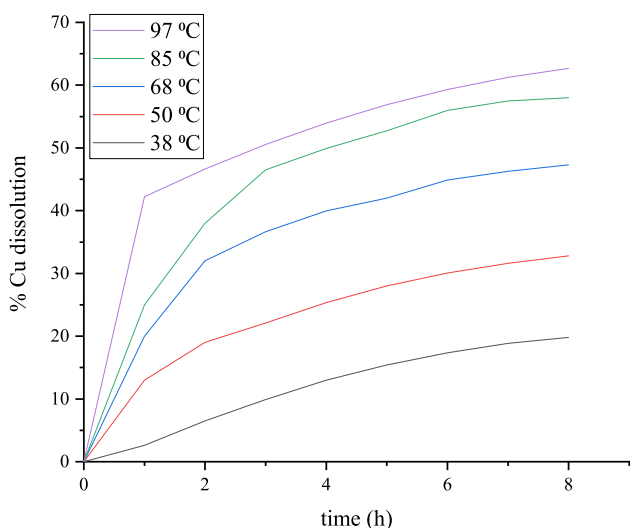


Fig. 8 Effect of temperature over copper dissolution (%) vs time (h) at 3 M HCl and [Cu²⁺] 0.5 M

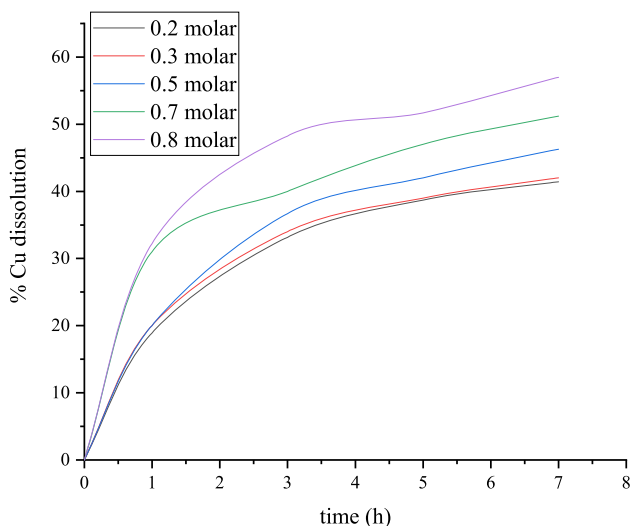


Fig. 9 Effect of cupric concentration over copper dissolution (%) versus time (h) at 3 M HCl and 68 °C

$$1 - \frac{2}{3}X - (1 - X)^{2/3} = kt \tag{12}$$

where k is the apparent reaction rate constant (h^{-1}), t is leaching time (h) and X is the fraction reacted.

This indicates that leaching of chalcopyrite under this condition is controlled by diffusion through the passivation layer and no external diffusion control or chemical control. Because of constant high stirring speed of 550 rpm, it can be concluded that external diffusion is eliminated but to investigate chemical control mechanism, the apparent activation energy has been calculated according to the Arrhenius equation $k = A \exp(-\frac{E_a}{RT})$ where k is reaction rate constant, A is the frequency factor, E_a is the apparent activation energy and R is the gas constant. It is shown in

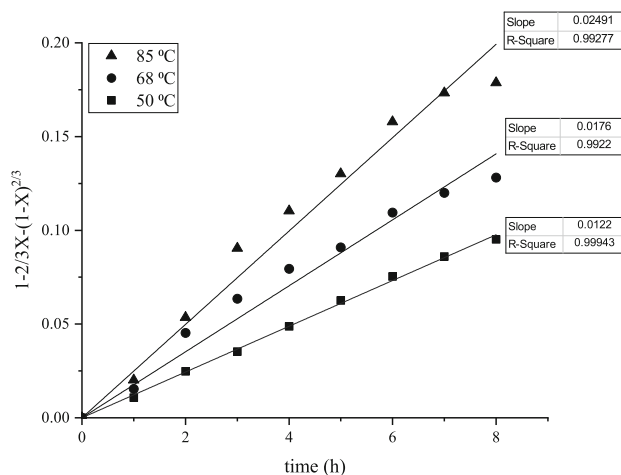


Fig. 10 Relationship between $1 - \frac{2}{3}X - (1 - X)^{2/3} = kt$ and leaching time at various temperatures

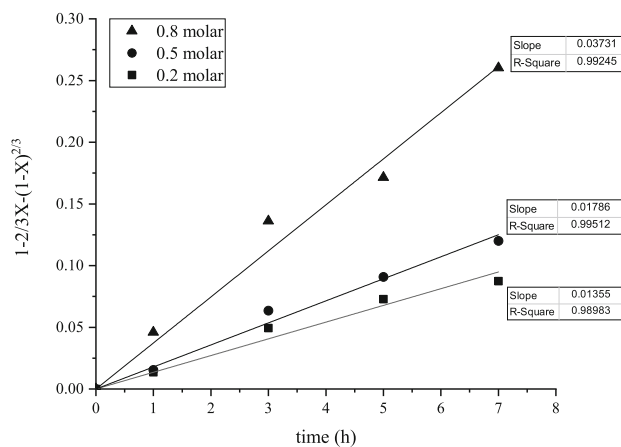


Fig. 11 Relationship between $1 - \frac{2}{3}X - (1 - X)^{2/3} = kt$ and leaching time at various cupric concentrations

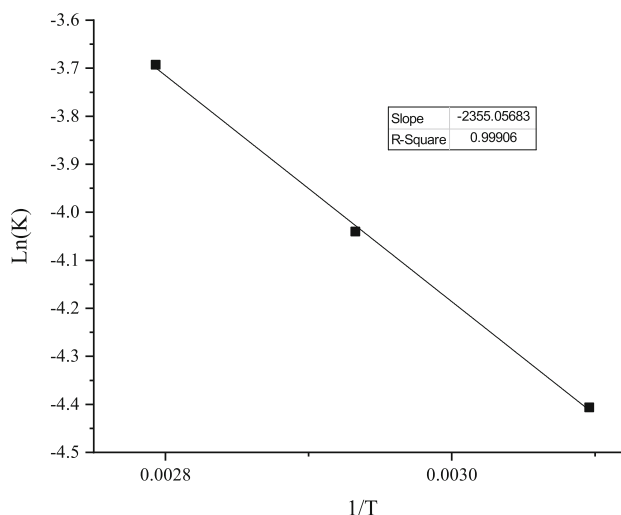


Fig. 12 Arrhenius plot for leaching of chalcopyrite

Fig. 12 that the plot of $\ln k$ to $1/T$ is linear with R -square of 99%, and E_a calculated from the slope is found to be 19.57 kJ/mol.

The typical activation energy for a chemically controlled mechanism is more than 40 kJ/mol, while the activation energy for a diffusion mechanism is less than 40 kJ/mol [28].

4 Conclusions

The effects of temperature, time and cupric ion concentration in constant particle size, pulp density, agitation speed and initial acidity of solution were investigated on oxidative leaching of chalcopyrite concentrate. The results indicated that cupric ion could be a helpful oxidant agent under experimental conditions. The following conclusions can be made from this study:

- (1) Temperature, time of holding and Cu^{2+} concentration had significant effect on the rate of leaching of chalcopyrite concentrate in chloride media.
- (2) Temperature had the greatest effect on copper and iron dissolution from chalcopyrite.
- (3) A model for dissolution of Cu was obtained according to Eq. 6 including all term with prediction correlation of 83.67%.
- (4) According to statistical analysis, the model was modified to a more predictable model shown in Eq. 7.
- (5) According to Pourbaix diagrams and stable areas of Cu^{2+} and Fe^{3+} , under experimental conditions, after 6 h dissolution of iron, it reduced because of increase in pH of solution.
- (6) The results of shrinking core model indicated that the process was controlled by diffusion through product layer represented as passivation layer.
- (7) The activation energy was determined to be 19.57 kJ/mol.

References

1. Córdoba E, Muñoz J, Blázquez M, González F, and Ballester A, *Hydrometallurgy* **93** (2008) 81.

2. Harmer S L, Thomas J E, Fornasiero D, and Gerson AR, *Geochimica et Cosmochimica Acta* **70** (2006) 4392.
3. Y'evenes L V, Miki H, and Nicol M, *Hydrometallurgy* **103** (2010) 80.
4. Veloso T C, Peixoto J J, Pereira M S, and Leao V A, *Int J Miner Process* **148** (2016) 147.
5. Pradhan N, Nathasarma K, Rao K S, Sukla L, and Mishra B, *Min Eng* **21** (2008) 355.
6. Hiroyoshi N, Arai M, Miki H, Tsunekawa M, and Hirajima T, *Hydrometallurgy* **63** (2002) 257.
7. Ahmadi A, Schaffie M, Petersen J, Schippers A, and Ranjbar M, *Hydrometallurgy* **106** (2011) 84.
8. Nicol M, and Lazaro I, in *5th Copper-Cobre International Conference*, 30 Nov–3 Dec 2003, Santiago, Chile.
9. Córdoba E, Nuevas evidencias sobre los mecanismos de lixiviación química y biológica de la calcopirita. Ph.D. thesis, Ph.D. Thesis. Universidad Complutense de Madrid (2005).
10. Tshilombo A F, Mechanism and kinetics of chalcopyrite passivation and depassivation during ferric and microbial leaching. Ph.D. thesis, University of British Columbia (2006).
11. Córdoba E, Muñoz J, Blázquez M, González F, and Ballester A, *Min Eng* **22** (2009) 229.
12. Viramontes-Gamboa G, Peña-Gomar M M, and Dixon D G, *Hydrometallurgy* **105** (2010) 140.
13. Arce E M, and González I, *Int J Miner Process* **67** (2002) 17.
14. Hackl R, Dreisinger D, Peters L, and King J, *Hydrometallurgy* **39** (1995) 25.
15. Olvera O, Rebolledo M, and Asselin E, *Hydrometallurgy* **165** (2016) 148.
16. Salehi S, Noaparast M, and Shafaie S Z, *Int J Min GeoEng* **50** (2016) 157.
17. Nicol M, and Zhang S, *Hydrometallurgy* **167** (2017) 72.
18. Lundström M, Liipo J, Taskinen P, and Aromaa J, *Hydrometallurgy* **166** (2016) 136.
19. Recalde E L, and Donoso P N, *J Mexican Chem Soc* **60** (2016) 238.
20. Cháidez J, Parga J, Valenzuela J, Carrillo R, and Almaguer I, *Metals* **9** (2019) 189.
21. Li Y, Kawashima N, Li J, Chandra A, and Gerson A R, *Adv Colloid Interface Sci* **197** (2013) 1.
22. Lu Z, Jeffrey M, and Lawson F, *Hydrometallurgy* **56** (2000) 189.
23. Watling H, *Hydrometallurgy* **146** (2014) 96.
24. Lundström M, Aromaa J, Forsèn O, Hyvärinen O, and Barker M H, *Hydrometallurgy* **77** (2005) 89.
25. Simpson J, Navarro P, and Alguacil F J, *Hydrometallurgy* **42** (1996) 13.
26. Habashi F, *Principles of Extractive Metallurgy*. Routledge, London (2017).
27. Sadrnezhad S, *Amir Kabir Pub Inst* (2004) 145.
28. Espiari S, Rashchi F, and Sadrnezhad S, *Hydrometallurgy* **82** (2006) 54.

Publisher's Note Springer Nature remains neutral with regard to jurisdictional claims in published maps and institutional affiliations.